AIP | Review of Scientific Instruments

Electron stripping processes of H− ion beam in the 80 kV high voltage extraction column and low energy beam transport line at LANSCE

I. N. Draganic

Citation: Review of Scientific Instruments **87**, 02B111 (2016); doi: 10.1063/1.4932398
View online: http://dx.doi.org/10.1063/1.4932398
View Table of Contents: http://scitation.aip.org/content/aip/journal/rsi/87/2?ver=pdfcov
Published by the AIP Publishing

Electron stripping processes of H⁻ ion beam in the 80 kV high voltage extraction column and low energy beam transport line at LANSCE

I. N. Draganic[a)]
Los Alamos National Laboratory, Los Alamos, New Mexico 87545, USA

(Presented 24 August 2015; received 21 August 2015; accepted 21 September 2015; published online 14 October 2015)

Basic vacuum calculations were performed for various operating conditions of the Los Alamos National Neutron Science H⁻ Cockcroft-Walton (CW) injector and the Ion Source Test Stand (ISTS). The vacuum pressure was estimated for both the CW and ISTS at five different points: (1) inside the H⁻ ion source, (2) in front of the Pierce electrode, (3) at the extraction electrode, (4) at the column electrode, and (5) at the ground electrode. A static vacuum analysis of residual gases and the working hydrogen gas was completed for the normal ion source working regime. Gas density and partial pressure were estimated for the injected hydrogen gas. The attenuation of H⁻ beam current and generation of electron current in the high voltage acceleration columns and low energy beam transport lines were calculated. The interaction of H⁻ ions on molecular hydrogen (H_2) is discussed as a dominant collision process in describing electron stripping rates. These results are used to estimate the observed increase in the ratio of electrons to H⁻ ion beam in the ISTS beam transport line. © *2015 AIP Publishing LLC.* [http://dx.doi.org/10.1063/1.4932398]

I. INTRODUCTION

Surface converter ion sources have been used successfully for production of the 800-MeV proton beam at Los Alamos National Neutron Science (LANSCE) for many years. The LANSCE negative ion source and its performance are well described elsewhere.[1,2] Typical extracted H⁻ ion currents are in the range of 14-16 mA at an extraction voltage of 80 kV. The low-energy beam transport (LEBT) line resides in the Cockcroft-Walton (CW) generator at high voltage (HV) (680 kV) which accelerates the beam up to a final energy of 750 keV trough a high-voltage column to a transport line at ground level. The negative ion source and CW injector are capable of operating at 60-Hz and 120-Hz repetition rates with pulse length of 835 μs. Achieving good vacuum conditions inside the ion source and in the high-voltage columns is critical for a stable and repeatable working regime of the injector with minimized interruptions due to HV arc discharges. The presented vacuum calculation results were used to understand an observed increase of electron current in HV electrostatic extraction column and signal noise seen in transverse beam emittance scans.

II. HIGH VACUUM SYSTEM

The ion source test stand (ISTS) reproduces the operational configuration of the negative ion source, electrostatic extraction column, and LEBT line in the dome of the production H⁻ CW injector. Figure 1 shows the ISTS configuration. High vacuum was produced by two turbo-molecular (TM) pumps (with pumping speeds PS1 = 2200 l/s and PS2 = 790 l/s) and a cryogenic pump (PS3 = 1500 l/s). An ultimate vacuum pressure of 2.0 to 8.0×10^{-8} Torr was achieved in the ISTS LEBT during described measurements. A residual gas analyzer was placed at the main chamber, and vacuum gauges were installed at three locations (main chamber, middle of LEBT, and end of LEBT). The characteristic reading of vacuum pressure was in the range of 3.0 to 9.0×10^{-6} Torr during a nominal ion source run. The recorded RGA mass spectra are shown in Fig. 2 indicate that molecular hydrogen is the dominant gas (98%–99%) in the LEBT. The corresponding pumping speeds for each pump for H_2 gas will be used in vacuum analysis presented below. There were no vacuum detectors on the HV column and ion source side. In order to understand the attenuation of the H⁻ ion beam and detect the origin of scattered electrons in emittance scans, we needed to perform a basic vacuum calculation inside the HV column taking into account all electrode apertures and beam component dimensions. A drawing of the 80 kV electrostatic extraction column design (i) with photos of four electrodes is shown in Figure 3. Each electrode has a centered hole for ion beam acceleration and additional openings for vacuum pumping (see photos ii–v in Fig. 3). The extraction (iii) and column (iv) electrodes in the H⁻ dome each have an additional set of three semicircular openings for improved pumping. These additional ports are not present in the ISTS extraction column. This small difference in electrode configuration between the ISTS and the production injector configuration motivated the calculation of increased vacuum pressure which may be a cause of H⁻ ion stripping on elevated gas densities and an origin of scattered electrons. Vacuum estimations were done for three different cases: (a) only centered holes included, (b) centered holes with outer large opening (ISTS column configuration), and (c) with all electrode holes included (H⁻ dome column configuration).

Note: Contributed paper, published as part of the Proceedings of the 16th International Conference on Ion Sources, New York, New York, USA, August 2015.

a)Author to whom correspondence should be addressed. Electronic mail: draganic@lanl.gov

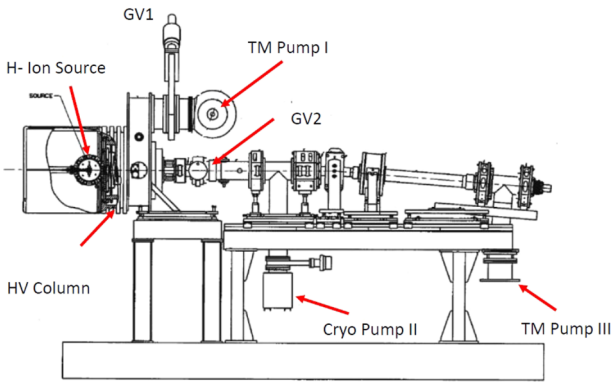

FIG. 1. Schematic view of H^- ion source test stand with three high vacuum pumps is shown.

III. VACUUM CALCULATIONS

An analysis of molecular gas flow for hydrogen in the extraction column at room temperature is presented below. Viscous and transition flow cases are omitted in this analysis. Based on detailed measurements and dimensions of all electrode orifices and vacuum line parts (main vessels, beam tubes, pipes, etc.), the vacuum conductance C (l/s) is calculated for each element. Total molecular flow conductance C_{tot} is summarized for each path between the point of interest (a-e) and each pump separately. The effective pumping speeds S_{eff} are estimated using pump speeds and flow conductance. For example, the effective speeds in the center of the main vacuum chamber are 1792 l/s, 242 l/s, and 99 l/s for pumps 1, 2, and 3, respectively. The first TM pump contributes to 84% of the effective pumping speed whereas pumps 2 and 3 have smaller contributions of 11% and 5%, respectively. The model does not consider contributions from vacuum leaks and wall outgassing rates. These mass flows are negligible to the injected hydrogen flow during normal operation of the H^- ion source. High purity hydrogen (99.99%) was injected as the working gas. Gas flow in the source was adjusted by fine-tuning flow meter in the range of 2.0–2.4 SCCM. The vacuum calculation was performed for the gas load of $Q = 2.67 \times 10^{-2}$ (Torr l/s) (or flow set point of 2.1 SCCM). Vacuum pressures are calculated using the formula $P = Q/S_{eff}$ (Torr) for all points of interests.

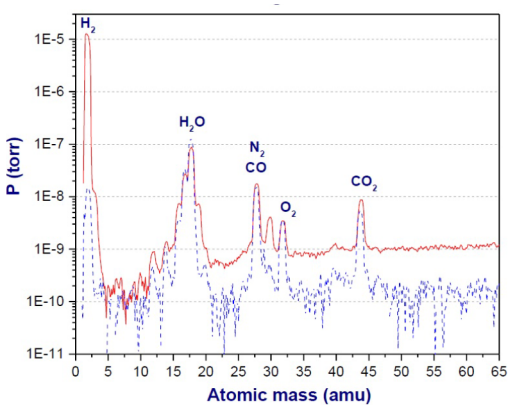

FIG. 2. Typical LEBT RGA mass scans recorded during maintenance (blue-dashed curve) and beam production period (red-solid line) with an identification of residual gas molecules.

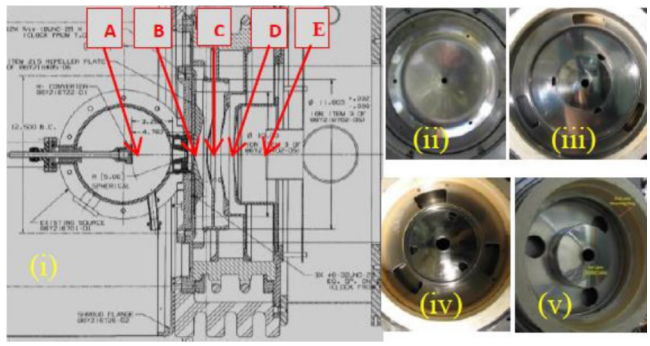

FIG. 3. (i) Cross section of HV electrostatic column with five points a-e where vacuum pressure was computed. The photos of the Pierce electrode (ii-b), the extraction electrode (iii-c), the column electrode (iv-d), and the ground electrode (v-e) are shown.

We have used the measured pressure near gate valve GV1 as a test of the vacuum model. When all three pumps were turned on, the achieved vacuum was $p = 7.3 \times 10^{-6}$ Torr. When the second valve GV2 at the LEBT was closed, with only the first pump on, the ion gauge reading was $p = 8.8 \times 10^{-6}$ Torr. Our model of vacuum system predicts H_2 corrected pressures of $p = 3.7 \times 10^{-6}$ Torr and $p = 4.6 \times 10^{-6}$ Torr, respectively. The final vacuum model results are shown in Figures 4–6. The effective pumping speeds in the HV column and ion source are presented in Figure 4. The effective speed changes from 8.8 l/s to 844 l/s from the ion source towards the column region. The model shows small differences in pumping speed between electrode configurations in the H^- dome and the ISTS. Differences in S_{eff} are also small when we have one or three pumps included because the first pump has the largest contribution to the total effective pumping speed. The effective speeds in point (a-d) are reduced from 4 to 15 times when only centered holes are included (black symbols). Working vacuum pressure inside the column is shown in Figure 5. Vacuum pressure changes from 3.0×10^{-3} Torr in the source to 3.0×10^{-5} Torr at the ground electrode end are noted. The electrode pumping ports lower the vacuum pressure by 50% in the source and reduce by an order of magnitude the vacuum

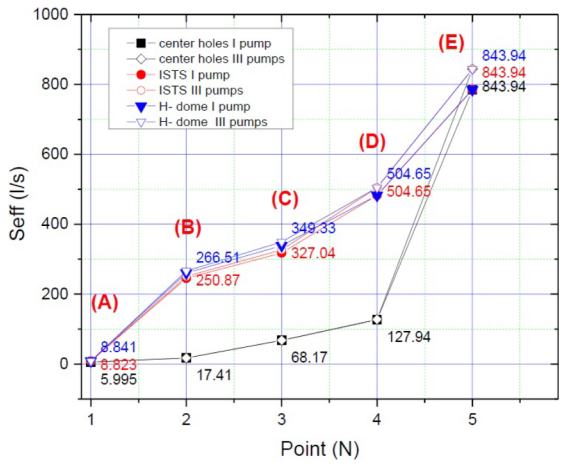

FIG. 4. Effective pumping speeds for different electrode configurations and points in the ion source and extraction column are presented. Symbols and filled symbols represent results for pumping with one or three pumps, respectively.

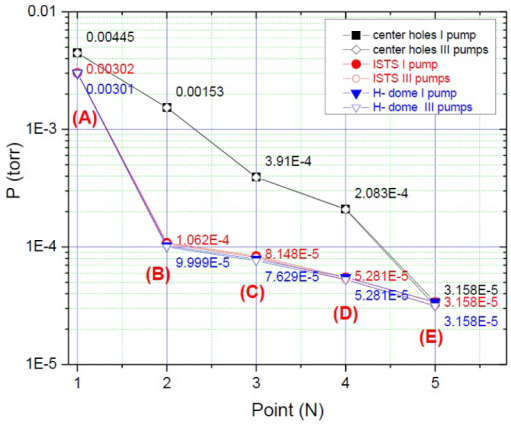

FIG. 5. Estimated vacuum pressure for different electrode configurations and points in the ion source and extraction column is presented. Symbols and filled symbols represent results for pumping with one or three pumps, respectively.

pressure between the Pierce electrode and extraction electrode where the highest gradient of electrical fields is applied. The same vacuum pressure in the range of 3 to 7×10^{-3} Torr in H^- source was previously observed.[3] The density of hydrogen gas inside the entire extraction column and source is presented in Figure 6. Neutral densities change by two orders of magnitude (from $n_{H2} = 1.0 \times 10^{-14}$ cm^{-3} to $n_{H2} = 1.0 \times 10^{-12}$ cm^{-3}). These estimated densities are used in the H^- beam attenuation calculation below.

IV. H^- ION BEAM STRIPPING PROCESS

The attenuation of extracted H^- ion beam is modeled using the atomic physics concept of the total cross section. The dominant collision process in our description of negative ion beam attenuation is the electron striping of H^- ion by molecular hydrogen. The total cross section data as a function of collision energy for this collision process $H^- + H_2 = e + H_2 + fast\ H$ are described in detail.[4] The fast accelerating beam traversing stationary collection of target particles (residual gases) will change as exponential form,

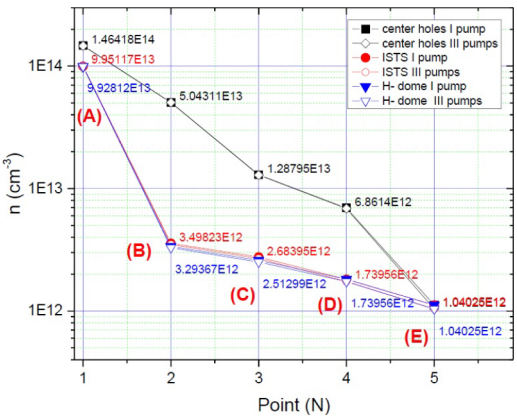

FIG. 6. Neutral particle densities for different electrode configurations and points in the ion source and extraction column are presented. Symbols and filled symbols represent results for pumping with one or three pumps, respectively.

TABLE I. H^- beam decay rate near electrodes along HV column.

Pressure of H_2 (Torr)	Density of H_2 (cm^{-3})	Δ I/I (%)
P_b = 1.06×10^{-4}	3.50×10^{12}	−0.87
P_c = 8.15×10^{-5}	2.68×10^{12}	−0.67
P_d = 5.28×10^{-5}	1.74×10^{12}	−0.43
P_e = 3.16×10^{-5}	1.05×10^{12}	−0.31
Total		−2.28

$$I(x) = I_0 e^{-\sigma n_b x}, \quad (1)$$

where I (x) is the remaining ion beam current at position x, I_0 is the initial beam current, n_b is the target particle density, and σ is the corresponding total cross section. The maximal total cross section of $\sigma = 1.0 \times 10^{-15}$ cm^2 for the projectile beam energies up to 80 keV is included. The distances between electrodes are 2.5 cm, i.e., total length between Pierce electrode and ground electrode is 10 cm. The densities for the residuals H_2 gas are shown in Fig. 6. The electron stripping rate of H^- ion beam on other residual gases (H_2O, O_2, N_2, CO, CO_2, etc.) is neglected because their partial pressures are two order of magnitude lower than the molecular hydrogen pressure (see Fig. 2). The electron stripping rate was analyzed for two main cases important for understanding the collision processes in the HV column. The first case corresponds to an electrode configuration in H^- dome that includes additional semi-circular pumping ports. The results are presented in Table I. The density of neutrals varies from 3.5×10^{12} cm^3 to 1.0×10^{12} cm^3 causing a total decrease of beam current of 2.28%. For the nominal beam current of 16 mA, electron stripping reduces the beam current by 0.38 mA. The same scattered electron current is generated. With a duty factor of 10%, such a newly generated electron beam will have a thermal power of 3 W. The electrons are insufficient to increase noise in emittance scans or to generate uncontrolled heat in the beam line comments, although past experiments have shown some elevated ISTS GV2 gate valve temperatures. The second case analyzed corresponds to an electrode configuration without additional pumping ports. Results show significant beam current drop of 17% and an increased density of neutrals up to 5.1×10^{13} cm^3. In this case, the electron beam has a power of 22 W that can cause heating downstream in the LEBT.

The method was used to compare with past H^- beam neutralization studies[5] that showed the extracted current can vary to −12.6%, when the column vacuum varies from 1.3×10^{-6} Torr to 1.1×10^{-5} Torr. Using presented method to estimate H^- beam current attenuation due to electron stripping process, a drop in current of −11.6% was predicted. This relatively good agreement proves our assumption that H^- stripping on H_2 is the dominant atomic process in H^- beam attenuation.

V. CONCLUSIONS

Vacuum estimation was made for the normal working regime of the ISTS and H^- dome extraction column. Calculated pressure variation at five different points of interest in main extraction column was presented for different configurations of holes on the high voltage column electrodes. The

vacuum pressure increases by a factor of 10 when side ports and openings for vacuum pumping are excluded. Vacuum pressure does not change between different electrode configurations at ISTS and H^- dome. The additional small holes do not contribute to the vacuum pressure in the 80 kV columns and will not significantly decrease extracted H^- beam intensity or generate scattered electrons.

ACKNOWLEDGMENTS

Author is thankful to the injector team members for providing data and photos of the production ion source and LEBT. This work is supported by the U.S. Department of Energy under Contract No. DE-AC52-06NA25396.

[1]J. Sherman *et al.*, "Physical insights and test stand results for the LANSCE H^- surface converter source," AIP Conf. Proc. **763**, 254 (2005).
[2]R. Keller *et al.*, "H^- ion source development for the LANSCE accelerator systems," AIP Conf. Proc. **1097**, 161 (2009).
[3]G. Rouleau *et al.*, Rev. Sci. Instrum. **79**, 02A514 (2008).
[4]T. Tabata and T. Shirai, "Analytical cross sections for collisions of H^+, H_2^+, H_3^+, H, H_2, and H^- with hydrogen molecules," At. Data Nucl. Data Tables **76**, 1–25 (2000).
[5]Y. Batygin *et al.*, "Space charge neutralization of H^- beam," TUPAW066, IPAC 2013, Shanghai, China.